

# Analytic Design of Slotless Brushless DC Motor with Hexagonal Windings

Jung-Moo Seo<sup>1,2</sup>, Young-Kyun Kim<sup>1</sup>, Se-Hyun Rhyu<sup>1</sup>, In-Soung Jung<sup>1</sup>, *Senior Member, IEEE*  
and Hyun-Kyo Jung<sup>2</sup>, *Senior Member, IEEE*

<sup>1</sup>Korea Electronics Technology Institute  
203-101 B/D 192, Yakdae, Wonmi, Bucheon, Gyeonggi, 420-140, Korea

<sup>2</sup>Seoul National University  
Gwanak \_ 1 Gwanakro, Gwanak, Seoul 151-742, Korea  
sjm@keti.re.kr

**Abstract** — An analytical model of slotless brushless DC motors having for-pole and twelve single coils is presented. To determine a back EMF constant of motor with hexagonal windings, winding forming factor taking into account a winding shape is introduced. The calculated results are verified with FE analysis through an example model, and electromagnetic parameters, such as EMF, motor constant with respect to the winding angle are analyzed.

## I. INTRODUCTION

Conventional structure of windings for slotless motors is rectangular shape which has the same coil pitch with respect to the axial length [1]. They can be analyzed in simple 2D FE method, however, the end-turn parts can be obstacle to combine with next windings and stator core in manufacturing process. This study presents analytic approach for design of the slotless motors which have hexagonal windings. Through air gap flux density and winding forming factor, back EMF constant is determined and derived results are compared with finite element analysis.

## II. BASIC CONFIGURATION

Fig. 1 shows a diagram of an inner rotor slotless BLDC motor which have four-pole, a double-layered full-pitch windings. A separated permanent magnet is used and a distributed winding composed of twelve single coils is fixed on the stator core. The maximum flux density of stator core is used for determine each parameters, such as inner stator core radius, outer PM and rotor radius, and air gap length. In magnetic circuit model taking into account one pole pair, the magnetic flux  $\Phi$  can be expressed as

$$\Phi = \frac{2R_m}{2R_m + 2K_r R_g} \Phi_r = \frac{1}{1 + K_r \frac{R_g}{R_m}} \Phi_r \quad (1)$$

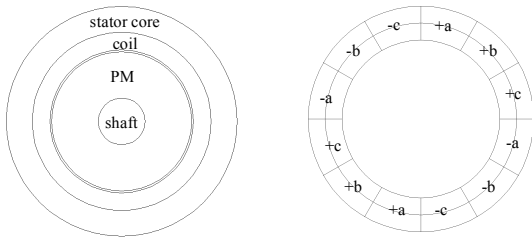


Fig. 1. Diagram of a slotless BLDC motor with a four-pole, double-layered twelve single coils.

where  $R_m$  and  $R_g$  are magnet and air gap reluctance respectively,  $\Phi_r$  is flux source, and  $K_r$  is reluctance factor which increases air gap reluctance slightly to compensate for the missing steel reluctance[2]. The air gap flux can be written as

$$\Phi_g = K_l \Phi = \frac{K_l}{1 + K_r \frac{\mu_r g A_m}{l_m A_g}} \Phi_r \quad (2)$$

where  $K_l$  is the flux leakage factor. The maximum flux density of stator core is

$$B_{sm} = \int_0^{\frac{\pi}{2}} \frac{\Phi_g \cos \theta}{A_{sc}} d\theta \quad (3)$$

where  $A_{sc}$  is surface area of stator core. In this study, the limitation of  $B_{sm}$  is set as 1.2T at no load condition and within the restriction the size of the PM is maximized as much as possible for achieving high torque density.

## III. EMF CONSTANT CALCULATION

Considering the flux linkage waveform which varies from a maximum positive value  $\Phi$  to a maximum negative value  $-\Phi$ , back EMF over half an electric cycle is given by

$$E = \frac{d\lambda}{dt} = \omega_e \frac{d\lambda}{d\theta_e} = p\omega_m \frac{2N\Phi_g}{\pi a} = K_e \omega_m \quad (4)$$

where  $\lambda$  is flux linkage and  $p$  is pole pair number,  $N$  is the number of conductors per phase, and  $a$  is the number of parallel paths. Using the winding coefficient  $K_w$ , the back EMF constant  $K_e$  can be expressed as

$$K_e = \frac{2pN\Phi_g K_w}{\pi a} \quad (5)$$

However, in hexagonal windings, actual flux linkage of a winding is different from conventional rectangular windings. It means that the surface area of hexagonal windings is smaller than rectangular one due to the diagonal regions of both the top and bottom sides. In a constant axial length, as the winding angle  $\theta_w$  is increased, surface area of windings  $A_w$  is decreased and coil width  $W_w$  is increased in Fig. 2 (a). Therefore, actual flux linkage in  $A_w$  and available number of conductors in coil region are controlled by  $\theta_w$ . Also  $K_e$  in (5) should be revised by introducing a winding forming factor  $K_f$ .

$$K_f = \frac{A_{w\_hexa}}{A_{w\_rect}} = \frac{(l_{ver} + l_{obq})l_{cir}}{l_{axi}l_{cir}} \quad (6)$$

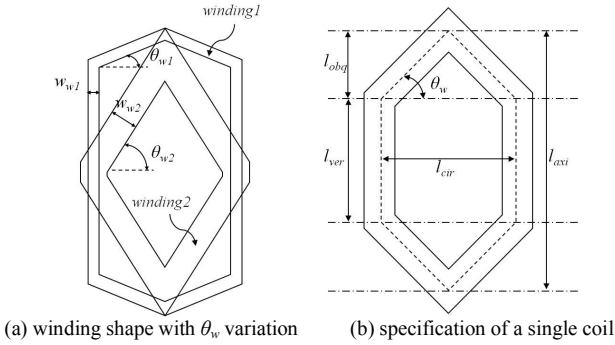


Fig. 2. Winding shape comparison and specification of a single coil. Surface area and coil width of winding are different with respect to the winding angle variation.

which  $A_{w\_hexa}$  and  $A_{w\_rect}$  are surface area of hexagonal and rectangular windings respectively,  $l_{xxx}$  is each winding length in Fig. 2 (b). Therefore  $K_e$  in slotless motor with hexagonal winding is expressed as

$$K_e = K_t = \frac{2pN\Phi_g K_w K_f}{\pi a} \quad (7)$$

#### IV. DESIGN EXAMPLE

Designed parameters of motor are presented in Table I. When an initial winding angle  $\theta_w$  is  $44.5^\circ$ , the calculated EMF constant is 0.0111Vs/rps from (7). 2D finite element analysis using slice region method is performed to verify the analytic results. Induced voltage of each slice region regarding diagonal shape of winding is determined and final EMF value is calculated considering overall axial length as follow [3].

$$E_{total} = E_k l_{ver} + 2 \sum_{n=1}^{k-1} E_n l_{obq} / (k-1) \quad (8)$$

where  $k$  is the number of slice region, and  $E_n$  is induced voltage of each slice region. EMF constant from above FEM simulation is 0.0110 Vs/rps which is good agreement with our model.

TABLE I. MOTOR PARAMETERS

Item	Value
Motor type	4 pole / 12 coil
Driving voltage [V]	24
Rated output power [W]	50
External diameter of stator yoke [mm]	21.0
Internal diameter of stator yoke [mm]	17.6
External diameter of PM [mm]	11.4
Internal diameter of PM [mm]	4.8
Axial length of stator core and PM [mm]	40
Air gap [mm]	0.4
PM remanency [T]	1.3 (sintered NdFeB)
Number of turns/phase	32
Winding angle [°]	44.5
Coil fill factor	0.7

As mentioned before, winding angle affects available coil fill area and winding forming factor. With above parameters in Table I, in order to investigate the relation among them, winding forming factor, winding width, EMF(torque) constant, and motor constant are calculated with respect to the winding angle variation in Fig. 3. Coil diameter and coil fill factor are assumed as the same value. Motor constant  $K_m$  is a figure of merit used to compare the relative efficiencies and output power capabilities of different motors.  $K_m$  defines the ability of the motor to transform electrical power to mechanical power, given by

$$K_m = \frac{T}{\sqrt{W_{in}}} = \frac{T}{\sqrt{I^2 R_t}} = \frac{K_e}{\sqrt{R_t}} \quad (9)$$

where  $W_{in}$  is input power and  $R_t$  is terminal resistance. In Fig. 3, increasing  $\theta_w$  decreases the  $K_f$ , which increase  $W_w$  as shown in Fig. 2 (a).  $K_m$  and  $K_e$  are increasing up to a certain winding angle, and then decreasing as angle increases. Also the maximum values of  $K_m$  and  $K_e$  are determined at different winding angle  $\theta_w$ . In a given structure of motors, the winding shape, or rather, winding angle is one of the main design parameters to decide motor characteristics.

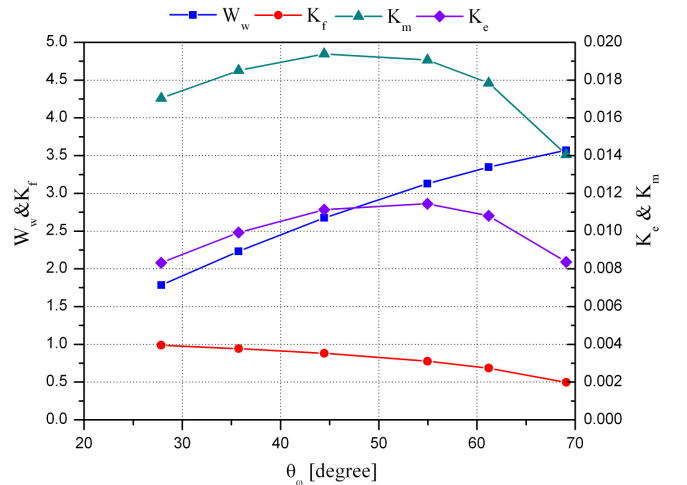


Fig. 3.  $W_w$ ,  $K_f$ ,  $K_m$ , and  $K_e$  variation with respect to  $\theta_w$ .

#### V. CONCLUSION

This paper presents an analytic method to design a slotless brushless DC motor. The proposed model can be applied to design conventional slotless motors and to predict static characteristics, torque efficiency using back EMF and motor constant with various winding shapes.

#### VI. REFERENCES

- [1] N. Bianchi, S. Bolognani, F. Luise "Analysis and Design of PM Brushless Motor for High-Speed Operations," *IEEE Trans. Energy conversion*, vol.20, no.3, pp.629-637, 2005
- [2] D. Hanselman, "Brushless Permanent Magnet Motor Design," second edition, The writers' collective, 2003
- [3] J. M. Seo, J. H. Kim, and I. S. Jung, "Design and Analysis of Slotless Brushless DC Motor," *IEEE Trans. on Industry Applications*, vol.47, no.2, pp.730-735, 2011